Electron transfer processes occurring on platinum neural stimulating electrodes: calculated charge-storage capacities are inaccessible during applied stimulation

Eric M Hudak[1,*,2,+], **Doe W Kumsa**[3,*,4,+], **Heidi B Martin**[1], and **J Thomas Mortimer**[3]

[1]Department of Chemical and Biomolecular Engineering, Case Western Reserve University, AW Smith Building, Cleveland, OH, USA

[2]Department of Research & Technology, Advanced Bionics LLC, Valencia, CA, USA

[3]Department of Biomedical Engineering, Case Western Reserve University, Wickenden Building, Cleveland, OH, USA

[4]Medical Device Innovation Consortium, St. Louis Park, MN, USA

Abstract

Objective—Neural prostheses employing platinum electrodes are often constrained by a charge/charge-density parameter known as the Shannon limit. In examining the relationship between charge injection and observed tissue damage, the electrochemistry at the electrode-tissue interface should be considered. The charge-storage capacity (CSC) is often used as a predictor of how much charge an electrode can inject during stimulation, but calculating charge from a steady-state i-E curve (cyclic voltammogram) over the water window misrepresents how electrodes operate during stimulation. We aim to gain insight into why CSC predictions from classic i-E curves overestimate the amount of charge that can be injected during neural stimulation pulsing.

Approach—In this study, we use a standard electrochemical technique to investigate how platinum electrochemistry depends on the potentials accessed by the electrode and on the electrolyte composition.

Main Results—The experiments indicate: 1) platinum electrodes must be subjected to a "cleaning" procedure in order to expose the maximum number of surface platinum sites for hydrogen adsorption; 2) the "cleaned" platinum surface will likely revert to an obstructed condition under typical neural stimulation conditions; 3) irreversible oxygen reduction may occur under neural stimulation conditions, so the consequences of this reaction should be considered; and 4) the presence of the chloride ion (Cl^-) or proteins (bovine serum albumin) inhibits oxide formation and alters H adsorption.

Significance—These observations help explain why traditional CSC calculations overestimate the charge that can be injected during neural stimulation. The results underscore how careful

---

Correspondence to: Eric M Hudak.

*former affiliation where experiments were conducted
+current affiliation

electrochemical examination of the electrode-electrolyte interface can result in more accurate expectations of electrode performance during applied stimulation.

Keywords

neural stimulation; neural prosthesis; platinum; charge-storage capacity; electron transfer; electrochemistry; electrochemical reaction; oxidation; reduction; redox; cyclic voltammetry; cyclic voltammogram; hydrogen adsorption

1. Introduction

Platinum has served as the go-to electrode material for neural stimulators because of its biocompatibility and long history of use in stimulating neural tissue for applications such as cochlear implants, deep brain stimulators, and spinal cord stimulators. Early on, neural prosthesis designers used platinum thinking it was an inert metal; serendipitously, it proved to be a reliable material that offered a relatively high charge-injection capability compared to many other biocompatible metals. However, for many devices, a limit has been imposed on platinum based on a charge/charge-density parameter first introduced by Shannon.[1] The Shannon limit intended to prevent stimulation at levels where unacceptable tissue damage may occur. The limit was based on observations of tissue damage from electrically-stimulated cat cortex by McCreery et al.[2] Although the underlying relationship between charge-injection level and observed tissue damage is not well understood, one important factor to consider is the production of electrochemical byproducts during stimulation. Researchers have investigated alternative electrode materials in order to stimulate tissue at higher magnitudes while avoiding certain electrochemical reactions presumed to be undesirable. Examples of these materials include iridium oxide, titanium nitride, tantalum oxide, carbon-based materials, rough or porous platinum/platinum-iridium, conductive polymers such as PEDOT and polypyrrole, and conductive hydrogels.[3–15] Very few of these alternative electrode materials have been successfully commercialized for a variety of reasons, including mechanical stability issues and lower charge capacity when applied to chronic implanted conditions.[8,16–19] By developing a more precise understanding of the electron-transfer processes on platinum, it may be possible to raise the traditional charge-transfer constraints imposed by the Shannon limit.

In the 1970s, Barry Brummer brought to light the importance of electrochemistry to the neural stimulation community and introduced the idea of "theoretical non-gassing limits" for stimulating electrodes.[20,21] Later referred to as the *charge-injection limit*, it is a measure of how much charge can be injected through a stimulating electrode before water electrolysis (H_2 or O_2 evolution) occurs, a phenomenon many believe to be damaging to tissue around an implanted electrode. Brummer and Turner calculated the charge available from the oxide reduction and hydrogen adsorption mechanisms on platinum using millisecond-scale current pulses, and predicted the amount of charge that could be reversibly injected with a cathodic-first pulse to be 350 $\mu C/cm^2$ (real area).[21] Later, Rose and Robblee determined how much charge could be injected with platinum electrodes during 200-μs neural stimulation pulses.[22] With the 200-μs pulses, their experiments showed that only 150 $\mu C/cm^2$ (geometric area) could be injected while avoiding potentials where H_2 or O_2 evolution could occur.

For an alternative estimate of how much charge an electrode is capable of transferring, Beebe and Rose began a trend of reporting the *charge-storage capacity* of electrode materials.[3] The charge-storage capacity (CSC) is calculated by first recording an i-E curve (i.e., current-potential curve, cyclic voltammogram) over the entire water window and then integrating the resultant current to provide a measure of how much charge an electrode can "store." The charge is divided by the electrode surface area to provide a charge density value. The cathodic CSC for platinum has been estimated to be as high as 550 **μC/cm²**.[23] CSC values are higher than charge-injection limits because they are recorded under slow rates of potential change. As a result, the electrochemical reactions have more time to run to completion before the edge of the water window is reached. CSC has become a popular way of comparing the charge-transfer capability of electrodes for neural stimulation, likely because it is much easier to determine compared to the more relevant charge-injection limit.

Through the experiments outlined in this communication, we aimed to better understand the primary mechanism of charge transfer on platinum electrodes, the atomic hydrogen (H) adsorption-desorption reaction, which occurs in the potential region just positive of H_2 evolution. As Brummer and Turner described, the adsorption and desorption of the hydrogen atom is a kinetically fast and highly reversible reduction-oxidation (redox) reaction, which makes platinum an attractive electrode material for neural stimulation.[20] The hydrogen adsorption-desorption reaction acts like a capacitor and is referred to as a pseudo-capacitance. This pseudo-capacitance operates in parallel with the double-layer capacitance to offer reversible electrochemical processes, which are widely accepted as safe mechanisms of charge injection because no electrochemical byproducts are produced in the reactions. The hydrogen adsorption-desorption reaction can occur on several noble metals [24]; the adsorption reaction for platinum is shown in equation (1.1).

$$Pt_{(s)} + H^+_{(aq)} + e^- \rightleftharpoons Pt\text{—}H_{(ad)} \quad (1.1)$$
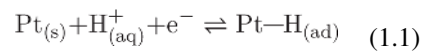
$H^+_{(aq)}$ represents a proton surrounded by water molecules (solvated hydronium), $Pt_{(s)}$ represents a specific site on the platinum surface, and e^- represents an electron transferred from the platinum electrode to the proton, as the electrode potential is decreased (i.e., polarized in the cathodic direction). $Pt\text{-}H_{(ad)}$ represents atomic hydrogen adsorbed to a single platinum surface site. There are a fixed number of Pt-H adsorption sites on the electrode surface and once all available sites are occupied, any additional cathodic electron transfer produces diatomic hydrogen (H_2).

The hydrogen desorption reaction on platinum is shown in equation (1.2). The electron transfers back to the metal as the electrode potential is increased (i.e., polarized in the anodic direction), and the proton is returned back to solution.

$$Pt\text{—}H_{(ad)} \leftharpoondown Pt_{(s)} + H^+_{(aq)} + e^- \quad (1.2)$$
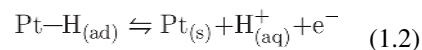
This hydrogen adsorption-desorption process is a type of faradaic reaction that is fully reversible because, in part, the reaction product is bound (chemisorbed) to the electrode

surface. The charge attributed to hydrogen adsorption is estimated to be 210 μC/cm^2 (real area) based on a likely distribution of crystal planes (predominantly the [100] plane) and assuming a monatomic layer of H atoms.[25–27] For a thorough discussion of the assumptions made in determining an H adsorption value of 210 μC/cm^2, see [27].

While conducting the studies reported in our previous communication [28], it became evident that in order to take full advantage of the hydrogen adsorption-desorption peaks shown in many platinum i-E curves in the neural prosthesis literature[23,29–33], repeated cycling of the interface potential over the full water window was necessary. Yet, when an electrode is in a living system, its characteristics more likely resemble those of the electrode on the initial cycle rather than the steady-state cycle. In this article, we analyzed i-E curves from the initial cycle to the steady-state cycle, focusing on the hydrogen adsorption reaction on platinum. In addition, an analysis of oxide formation and the effects of chloride ions and proteins on H adsorption is presented. The objective is to gain insight into why CSC predictions from classic platinum i-E curves overestimate the amount of charge that can be injected during neural stimulation pulsing.

2. Experimental materials and methods

i-E curves were recorded on platinum wire and platinum disk electrodes in sulfuric acid solutions. In the first set of measurements (figures 2–5), the working electrode was a platinum wire (Goodfellow, 99.998%, as drawn, #PT005141) with a geometric surface area of 44×10^{-3} cm^2 (0.25-mm diameter, 5.5-mm exposed length) and a large platinum mesh counter electrode. The surface area was calculated assuming the exposed wire was a smooth cylinder with one flat, disk-shaped end (all reported charge density values were calculated with this geometric area). In the second set of measurements (figures 6 and 7), the working electrode was a platinum disk (eDAQ, 99.5%, #ET075-1) with a geometric area of 7.8×10^{-3} cm^2 and the counter electrode was a carbon rod. The counter electrodes differed in each set of measurements due to availability at the time of the experiment. Since the surface areas of the counter electrodes were very large in comparison to the working electrodes, they did not have any effect on the electrochemical reactions occurring at the working electrode surface. All potentials were measured with respect to a Ag|AgCl (3 M NaCl, 0.209 V vs. SHE) reference electrode (BASi, #RE-5B). Prior to each experiment, the working electrode, counter electrode, and reference electrode were rinsed thoroughly with deionized, distilled water.

The 0.15 M H$_2$SO$_4$ electrolyte was prepared by diluting concentrated sulfuric acid (Fisher Scientific; Certified ACS Plus†, #A300S) with deionized, singly-distilled water (not ultrapure). In certain experiments, 0.15 M NaCl (Fisher Scientific, Certified ACS, #S271-3) or bovine serum albumin (BSA) solution was added to the sulfuric acid electrolyte. The BSA solution was prepared by dissolving BSA powder (Sigma-Aldrich, #A2153) into 0.15 M NaCl at a concentration of 0.2 mg/mL.

---

†Certified ACS and Certified ACS Plus are Fisher Scientific designations indicating the reagent meets or exceeds the latest specifications of the American Chemical Society. Certified ACS Plus reagents are also analyzed for more than 16 trace metals.

While dilute sulfuric acid may seem to have little resemblance to the fluids surrounding an electrode in a living system, it is an excellent medium to study the basic properties of a platinum electrode. Both a sulfuric acid electrolyte and all living systems share the common components of protons, hydroxide ions, and water molecules. Also, even with careful preparation of sulfuric acid electrolytes, there will be organic molecules (contaminants) in solution that affect the electrochemistry, as is the case in a living system. The utility of sulfuric acid as an electrolyte for neural stimulation studies is further discussed in section 4.1.

The electrochemical cell was a cylindrical dish (Corning Pyrex, #3140-70) filled with 100 mL of electrolyte and covered with laboratory film (Parafilm M). The electrodes and a gas sparging tube were inserted into the cell through small holes in the film. Before i-E curves were recorded, the electrolyte was bubbled for 30 minutes with either N_2 (Airgas, Ultra High Purity 99.999% N_2) to minimize dissolved oxygen or O_2 (Airgas, Ultra High Purity 99.994% O_2) gas to maximize dissolved oxygen in the electrolyte. Gas was continuously passed over the electrolyte surface for the duration of the experiment to maintain a constant (saturated) dissolved gas composition.

i-E curves were recorded at a scan rate of 100 mV/s using a Bio-Logic VSP® potentiostat (figures 2–5) and an Autolab PGSTAT128N potentiostat with the linear scan generator module SCAN250 (figures 6 and 7). Charge was calculated from the i-E curves in figures 2–5 using the "Integral" function of the Bio-Logic EC-Lab V9 software, which uses a trapezoidal rule to integrate the current-versus-time data. Platinum i-E curves were compared for two potentials ranges: in the conventional 1.5-volt water window (approximately −0.25 V to +1.25 V vs. Ag|AgCl) and in a narrower window (approximately −0.25 V to +0.55 V vs. Ag|AgCl). The upper potential limit of the water-window i-E curve was limited to +1.25 V vs. Ag|AgCl to avoid generating O_2 at more positive potentials, which would have compromised the deoxygenated (N_2-saturated) electrolyte. The narrower window will be referred to as the *potential window for stimulation*, with the upper limit approximately at the OCP.

When an electrode is submerged in an electrolyte, it stabilizes at OCP until an experiment is started. In figure 1, the range of OCPs on one platinum electrode from several experiments in N_2-saturated and O_2-saturated 0.15 M H_2SO_4 versus an Ag|AgCl (3 M NaCl) reference electrode is shown. The mean OCP values were 0.60 ± 0.038 V for N_2-saturated electrolyte and 0.76 ± 0.023 V for O_2-saturated electrolyte (see table 1). The mean OCP values are indicated by a dashed vertical line in figures 2–5.

3. Results

3.1. Steady-state i-E curve over the water window

A steady-state i-E curve for a platinum electrode in N_2-saturated 0.15 M H_2SO_4 over the entire water window (−0.25 V to +1.25 V vs. Ag|AgCl) is presented in figure 2a. The potential was swept at a constant rate of 100 mV/s between the positive and negative limits while the current was being recorded. For a comprehensive explanation of the theory behind i-E curves (or i-V_e profiles, cyclic voltammograms) and how to record and interpret them,

see our previous publication.[34] Typical platinum behavior was indicated by the observed current peaks: oxide formation and reduction, atomic hydrogen (H) adsorption and desorption, and molecular hydrogen (H_2) evolution and desorption. For the i-E curve in figure 2a, the cathodic charge transfer associated with double-layer charging and the hydrogen adsorption reactions in the region between −0.22 V and +0.05 V (blue shaded area) was calculated to be 698 μC/cm^2. This indicates a roughness factor of about 3, assuming a monolayer of adsorbed atomic hydrogen corresponds to 210 μC/cm^2.[26,27,35]

In figure 2b, the steady-state i-E curve for a platinum electrode in O_2-saturated 0.15 M H_2SO_4 over the entire water window is shown. In the O_2-saturated environment, at potentials negative of the OCP (+0.76 V), platinum reduces dissolved O_2 molecules to form the superoxide radical ($O_2^{\bullet-}$) [36–38] or other species like H_2O_2. This reduction reaction provides a source of negative current that shifts the i-E curve downward in this potential range. The upper limit of the i-E curves in figure 2 was chosen to be +1.25 V to prevent the formation of molecular oxygen (O_2), which occurs at potentials above this limit.

3.2. i-E curves in the potential window for stimulation

Shown in figure 3a is an i-E curve of a platinum electrode scanned from the mean OCP to the negative limit of the water window (approximately +0.55 V to −0.25 V) for 100 cycles in N_2-saturated H_2SO_4. Cycling through this potential range more accurately reflects the primary potential window platinum electrodes encounter during neural stimulation pulsing. Prior to initiating this sequence of i-E curves, the as-manufactured electrode had been stored in air, rinsed with deionized distilled water, then submerged in the N_2-saturated electrolyte. In the first cycle (bold gray trace), hydrogen (H) adsorption-desorption peaks were relatively undefined compared to the same region (approximately −0.22 V to +0.05 V) in figure 2a when scanning over the wider window (−0.25 V to +1.25 V). At the negative end of the i-E curve, molecular hydrogen (H_2) is formed from the reduction of water molecules. In cycle 2 (first of the thin black traces), the cathodic charge density associated with double-layer charging and hydrogen adsorption was 438 μC/cm^2.[‡] As scanning progressed, the current associated with hydrogen adsorption steadily decreased, and by the 100th cycle (bold black trace; deemed as steady-state), cathodic charge density had decreased to 326 μC/cm^2. A similar decrease in hydrogen adsorption current was observed in O_2-saturated sulfuric acid (figure 3b).

3.3. i-E curves over the water window expose sites for hydrogen adsorption

After the 100th cycle of figure 3a, the electrode was then scanned over the entire water window (−0.25 V and +1.25 V), and the resulting i-E curves are shown in figure 4a. By polarizing the electrode through the oxide formation region (> +0.55 V) repeatedly, charge transfer in the hydrogen (H) adsorption/desorption region gradually increases over time. By the 50th cycle (bold black trace), the i-E curve has reached a steady state, and the hydrogen adsorption-desorption peaks became well defined. The cathodic charge in the hydrogen

---

[‡]*Note on charge density values:* Some charge densities reported in this article are higher than those calculated from platinum I-E curves in other literature. Possible explanations include: 1) a very rough electrochemical surface area and 2) insufficient adhesion between the insulating polymer and the platinum metal, hence a larger-than-intended exposed surface area. Whatever the cause of these high charge densities, the overall observed trends and conclusions are still valid.

adsorption region (−0.22 V to +0.05 V) in the last cycle, deemed the "cleaned state," was calculated to be 698 $\mu C/cm^2$. This last cycle is the i-E curve presented in figure 2a.

The i-E curve of platinum in O_2-saturated H_2SO_4 between −0.25 V and +1.25 V is shown in figure 4b. Similar to the N_2-saturated case, as cycling over the entire water window progressed, the H adsorption current increased to a steady-state value within 50 cycles. This last cycle is the i-E curve presented in figure 2b.

3.4. i-E curves in the window for stimulation after scanning through the oxide region

In figure 5a, i-E curves for the same platinum electrode in N_2-saturated H_2SO_4 immediately after the electrode had been cycled through the oxide formation region to a steady state (after 50th cycle in figure 4a) are shown. In the first cycle (bold gray trace) over the narrower potential window, the charge density for H adsorption was 690 $\mu C/cm^2$. As scanning progressed, however, the current associated with H adsorption steadily decreased. Charge transfer in the H adsorption region decreased from 690 $\mu C/cm^2$ to 435 $\mu C/cm^2$ by the 100th cycle (bold black trace). Comparing this to the fully developed electrode represented in figure 4a, there was about a 38% decrease in H-adsorption charge transfer when operating platinum in the narrower window.

i-E curves of the platinum electrode in O_2-saturated H_2SO_4 over a sequence of 100 cycles in the narrow potential window (immediately after the 50th cycle in figure 4b) are presented in figure 5b. Over the progression from the first cycle (gray) to steady state (black), the current associated with H adsorption decreased similarly to the N_2-saturated case.

3.5. The effect of chloride ions and proteins

Beyond the protons, hydroxide ions, water molecules, and dissolved O_2 studied in diluted sulfuric acid, two important components of living tissue should be considered when analyzing electrodes for neural stimulation: proteins and chloride ions (Cl^-). Both can have significant effects on the electrochemical activity of the electrode and may alter the amount of charge that can be injected from platinum.

Previously, we have shown that phosphate-buffered saline electrolytes may provide inaccurate electrochemical results since the phosphate groups are electrochemically active in certain potential regions.[28] So, we attempted to evaluate the electrochemical response of platinum in an unbuffered saline solution as a vehicle for examining the effect of Cl^-. i-E curves of a platinum disk electrode in 0.15 M H_2SO_4 (black trace) and in unbuffered 0.15 M NaCl (blue traces) are overlaid in figure 6. Several visual differences between i-E curves in the two electrolytes are apparent. One major difference is that the sulfuric acid i-E curve achieved a stable steady state, whereas the unbuffered NaCl i-E curves continually changed over time. The oxide reduction current decreased with time and an additional small reduction peak began to appear near +0.50 V (see red arrows). There was also a difference in the apparent water window of platinum in these electrolytes. The negative limit of the i-E curves in unbuffered NaCl is shifted 0.55 V negative of the i-E curve in sulfuric acid. This shift is due to the difference in pH between sulfuric acid (pH = 0.9) and unbuffered NaCl (pH ~ 7, unstable).[39] The overall width of the water window was larger in unbuffered NaCl (1.8 V) than in sulfuric acid (1.5 V). Also, the shapes and amplitudes of the hydrogen

adsorption-desorption peaks differ. The differences observed between dilute sulfuric acid and unbuffered NaCl may be explained by variations in pH [39,40] and ion adsorption effects, which are further studied below. Because of the instability of the i-E curve in unbuffered NaCl, it is not normally used as a test electrolyte for careful analyses of platinum (or other metal) electrochemistry. As discovered previously, even phosphate-buffered NaCl electrolytes exhibit electrochemical reactions that may not occur in vivo.[28]

In a related experiment, a platinum electrode in sulfuric acid was first scanned through the water window until steady state was reached (figure 7a, black trace). Then, aliquots of 0.15 M NaCl were added to determine how the chloride ion (Cl^-) affects the electrochemical activity. Upon addition of 1 mL of the NaCl electrolyte (final NaCl concentration of approximately 3 mM) and cycling to steady state, the current response for oxide formation decreases in the potential range from +0.55 V to +0.90 V, but appears relatively unchanged above +0.90 V. Also, the relative amplitudes of the hydrogen adsorption peaks change. Addition of 5 mL NaCl (final concentration of approximately 15 mM) resulted in an additional reduction in oxide formation current, and slight changes to the hydrogen adsorption peaks.

Further insight on the behavior of platinum electrodes can be gained from the work by Robblee et al.[41] Robblee showed that under pulsed conditions, less platinum was detected in solution when human serum albumin (a protein) was added to a phosphate buffered saline electrolyte (i.e., less platinum dissolution occurred). To gain a better understanding of this observation, bovine serum albumin (BSA) solution was added incrementally to sulfuric acid electrolyte and its effect was observed (figure 7b). Serum albumins are globular proteins and human serum albumin is a prominent constituent of cerebrospinal fluid. Shown in figure 7b, a 1-mL addition of BSA solution results in current suppression over most of the oxide formation region (+0.55 V to +1.20 V) Additional amounts of BSA (up to 9 mL) did not result in a significant further change in the i-E curve. The approximate final concentrations of BSA in solution for the 1, 2, 5, and 9-mL additions were 4, 8, 20 and 36 μg/mL, respectively. With BSA and other organic molecules, the suppression of oxide formation and H adsorption has been reported as an overall surface blocking effect,[42,43] where the organic molecules physically block platinum surface sites from participating in redox reactions.

4. Discussion

The i-E curve (slow-scan cyclic voltammogram) provides information about the electron-transfer processes that are thermodynamically possible on a stimulating electrode, and they should be consulted by neural prosthesis engineers to understand the possible consequences of permitting specific electrode potential excursions. The results of the experiments performed here indicate: 1) platinum electrodes must be subjected to a "cleaning" procedure in order to expose the maximum number of surface platinum sites for hydrogen adsorption; 2) the "cleaned" platinum surface will likely revert to an obstructed condition under typical neural stimulation conditions; 3) irreversible oxygen reduction may occur under neural stimulation conditions, so the consequences of this reaction should be considered; and 4) the

presence of the chloride ion (Cl⁻) or bovine serum albumin (BSA) inhibits oxide formation and alters H adsorption.

4.1. Sulfuric acid as a model electrolyte

In this study, dilute sulfuric acid was used as the electrolyte for platinum because it is a relatively well-understood electrochemical electrode-electrolyte system. Also, it contains protons, hydroxide ions, and water molecules, all of which are present in any living system. Protons and hydroxide ions are present in both sulfuric acid and in vivo, although in different proportions, giving rise to a pH difference and the resulting shift in potential. The sulfate (SO_4^{2-}) and bisulfate (HSO_4^-) anions in sulfuric acid adsorb to the platinum surface, but do not have a significant inhibiting effect on oxide formation or hydrogen (H) adsorption.[42,44–46] Understanding the electron transfer processes involving protons and water provides the basis for adding other candidate reactants to the test electrolyte. In our experiments in unbuffered NaCl, it was not possible to obtain a well-developed and stable i-E curve that can be used as a standard (see figure 6). In our previous study in phosphate-buffered saline, it was clear that the phosphate components can be electrochemically active. [28] However, in a sulfuric acid electrolyte, a stable i-E curve could be achieved relatively easily and its characteristics matched very well to platinum/sulfuric-acid i-E curves in literature.[43,47–51] This stable curve provides a baseline electrochemical response of platinum to which other test components can be added to solution for analysis.

4.2. The OCP and the effect of oxygen (O_2) reduction

When an electrode is submerged in an electrolyte, the electrode potential stabilizes at the point (known as a mixed potential) where current for cathodic processes is balanced with current for anodic processes, resulting in zero net current across the interface. This stable point is called the open-circuit potential (OCP). For an electrolyte containing O_2, current for O_2 reduction (a cathodic process) is balanced with current from anodic processes. Hoare et al. deduced that the OCP is a mixed potential arising from oxygen reduction and platinum oxide formation reactions.[52] An analysis by Rand and Woods showed that the likely anodic processes were platinum dissolution and oxidation of organic contaminants ("impurities") in solution.[47] Without O_2 present, there is no cathodic current from oxygen reduction, so the electrode rests at a more negative potential because the electrode must find a cathodic process with which to balance the anodic current from dissolution and organic oxidation. This shift was observed in our experiments (see figure 1 and table 1), where the OCP in O_2-saturated electrolyte was positive (anodic) to the OCP in deoxygenated electrolyte. In this study, O_2 reduction was observed at all potentials negative to the OCP when O_2 was present. With cathodic-first neural stimulation starting from OCP, the electrode will travel through this potential region where O_2 reduction is thermodynamically favorable. Therefore, future electrochemical studies relating to neural stimulation should consider an O_2 concentration near that found in neural environments (~5%).[53] The consequences of oxygen reduction can be the generation of reactive oxygen species, such as superoxide and hydrogen peroxide, which may not be reversible upon the application of the positive phase of the biphasic pulse. Superoxide radicals are known to react with nitric oxide (NO) to form peroxynitrite, which can be toxic to cells in the vicinity of the stimulating electrode.[54–56] Because NO is a prominent vasodilator, depletion of this molecule through the reaction with

superoxide may result in vessel constriction near neural tissue. However, reactive oxygen species are also a consequence of normal metabolic processes and scavengers are naturally present to mitigate them.

4.3. Hydrogen adsorption is dependent on the potential range

When a platinum i-E curve appears in a publication concerning neural stimulation, it is almost always a steady-state i-E curve in an oxygen-free electrolyte, as shown in figure 2a. It is important to realize that, prior to recording this i-E curve, the electrode potential had been swept many times over the entire potential range shown on the potential scale, as shown in figure 4a. With each sweep cycle, more and more charge can be reversibly transferred across the electrode interface until little or no increase is observed with additional cycling. The i-E curve at the end of the cycling process is referred to as a steady-state i-E curve or steady-state cyclic voltammogram (CV). Reaching this steady state takes several minutes of cycling, whereas a neural stimulation pulse may only last microseconds. In the case of figure 4, the electrode was cycled over the −0.25 V to +1.25 V range fifty times. Such a sweeping or cycling procedure, sometimes referred to as *cleaning* the electrode, is not often discussed in the neural prosthesis literature, and that absence can be misleading to a novice. After sweeping the potential over the −0.25 V to +1.25 V range fifty times, the charge stored in the hydrogen adsorption region increased from ~400 $\mu C/cm^2$ to ~700 $\mu C/cm^2$. Sweeping the potential over the −0.25 V to +0.55 V range did not improve the CSC of the hydrogen adsorption reaction (figure 3a). Comparing the results obtained from figure 3 with those of figure 4, it is apparent that to achieve the enhanced charge storage of hydrogen adsorption, the electrode potential needs to be swept through the platinum oxide formation region. Further, as shown in figure 5, the cleaned or enhanced hydrogen adsorption region cannot be maintained if the electrode potential is not swept into the range where oxide is formed.

One might think of applying an anodic bias to the electrode prior to the application of a cathodic neural stimulation pulse to develop surface sites for hydrogen adsorption. The results of these experiments suggest that this may not enhance charge transfer unless the positive bias was applied repeatedly (or for long periods of time) and that some of the exposed sites may be blocked during the inter-pulse interval. Applying an anodic bias on platinum may have other consequences in vivo such as enhanced corrosion through the formation of platinum-chloride complexes.[20,57–59]

In the electrochemistry literature of the 1950s and 60s, several investigators reported altered electrochemical activity on platinum depending on the potential range accessed by the electrode. Out of these observations, two theories on the cause of the activity changes arose: 1) scanning through more positive potentials oxidizes contaminants or organic materials in the electrolyte that had adsorbed to the electrode surface, thus freeing surface sites for charge transfer [60–63] and 2) scanning into the oxide formation potential region elicits "activation" of the platinum surface, producing a layer of more active platinum sites [64–68]. French and Kuwana estimated that the activated state would revert to the inactivated state with a half-life of 46 minutes.[68] More recently, Hibbert et al. demonstrated the inhibition of hydrogen adsorption by cycling a platinum electrode in a phosphate buffered saline electrolyte containing the protein human serum albumin (HSA) and/or amino acids.

[31] From our review of literature, a consensus on the true cause of hydrogen adsorption inhibition never developed. Regardless of the cause, the implications for this activity change are clear. During neural stimulation, if the platinum electrode is mostly exposed to potentials negative of OCP, then the electrode will not be able to transfer as much charge as it would if the surface had been fully "activated" or "cleaned of contaminants" by cycling through the entire oxide formation region.

4.4. Chloride ions and proteins adsorb to the platinum surface

The protons, hydroxide ions, and water molecules in sulfuric acid are not the only components to consider when evaluating the electrochemistry of a stimulating electrode. One significant ion present in the body is the chloride ion (Cl^-). Adding chloride (0.15 M NaCl) to the sulfuric acid electrolyte (figure 7a) demonstrated that the presence of Cl^- decreases the overall amount of oxide formation and alters the relative peak heights for H adsorption-desorption. Several researchers have investigated ion adsorption on the platinum surface.[42,48,69,70] Bagotzky et al. demonstrated that Cl^- adsorbs to the surface and changes the energy distribution of H adsorption, but does not decrease the amount that occurs (a full monolayer of H can still be adsorbed). Novak and Conway demonstrated that the adsorption of Cl^- acts to suppress oxide film formation.[48] When Cl^- is adsorbed, it can be oxidized through the corrosion reaction in (4.4.1).

$$Pt_{(s)} + 4Cl^-_{(ad)} \leftrightharpoons [PtCl_4]^{2-}_{(aq)} + 2e^- \qquad (4.4.1)$$

$$E = +0.49 \text{ V vs. Ag|AgCl (at 25 °C, 1 atm, pH} = 0.9)$$

Another aspect of living tissue that will affect the electrochemical performance of an electrode is the presence of organic materials like proteins. The experiment in figure 7b demonstrated that BSA suppresses oxide formation and alters H adsorption. Evidence in literature demonstrates that BSA readily adsorbs to the platinum electrode surface.[71] Bagotzky et al. found that when organic molecules adsorb to the surface of platinum, both oxide formation and the amount of H adsorption decrease.[42] The suppression of oxide formation current in figure 7b indicates that BSA is blocking the platinum surface from being fully oxidized.[43] By examining the H *desorption* (positive) peaks in figure 7b, it is apparent that less H adsorption had happened when BSA was present. It has also been shown that organic molecules and anions compete for surface sites when adsorbing on platinum.[42] When both BSA and chloride are present, BSA may occupy surface sites to which chloride ions would otherwise adsorb. With less chloride adsorbed, the corrosion reaction above would be suppressed. Robblee measured decreased platinum corrosion products with the addition of human serum albumin to phosphate buffered saline.[41]

Even with high-quality reagents and deionized distilled water, contaminants may be present in solution that can affect electrochemical measurements. Most would consider the sulfuric-acid-only i-E curves in figures 6 and 7 as "textbook" i-E curves of platinum in sulfuric acid. Specifically, the pronounced hump at the beginning of the oxide formation region (+0.55 V

to +0.9 V), the well-centered double-layer region (near +0.1 V), and the sharp H adsorption-desorption peaks (−0.22 V to +0.05 V) are all indicative of a high-purity de-oxygenated electrolyte and a pure platinum electrode that has been scanned to steady state. Its characteristics are very similar to i-E curves of platinum in sulfuric acid presented in other literature.[43,47,48,72] The slow rise of oxide formation current in the sulfuric acid i-E curve in figure 2a, however, may indicate that organic contaminants were present in the sulfuric acid electrolyte used in figures 2–5. In those experiments, ultrapure water was not used to prepare the electrolyte and paraffin film was used to cover the electrochemical cell, both of which are possible sources of organic contamination. Note the similarity in the shape of the oxide formation shoulder (+0.55 V to +1.2 V) in figures 2a (possible organic contaminants) and 7b, where organics (BSA) were intentionally added to solution. That observation supports the theory that scanning through more positive potentials (as demonstrated in figure 4) oxidizes organic molecules on the electrode surface, thus freeing surface sites for charge transfer via the hydrogen (H) adsorption reaction.

5. Conclusions

The results of this study help to explain why charge densities predicted from platinum steady-state i-E curves are not achievable during neural stimulation-type pulses. Charge (i.e., number of electrons) transferred via the hydrogen adsorption reaction on platinum greatly depends on the availability of surface adsorption sites. Without subjecting platinum to a "cleaning" procedure, surface sites are blocked and unavailable for hydrogen adsorption. Further, a "cleaned" surface reverts to a compromised surface relatively quickly.

For an as-manufactured electrode scanned from OCP toward hydrogen evolution, the charge density in the H adsorption region was only 326 $\mu C/cm^2$. Larger charge densities were only achieved if the electrode was scanned through more positive potentials in the oxide formation region. After cycling a platinum electrode over the entire water window (between −0.25 V and +1.25 V) for 50 cycles, the maximum charge density over the H adsorption region was 698 $\mu C/cm^2$. Further, once "activated" or "cleaned," if the electrode potential was not driven positively into the platinum oxide formation region, the electrode reverted to the state where decreased H adsorption occurs. It was also shown that both the chloride ion (Cl^-) and protein molecules (BSA) adsorb to the platinum surface and independently decrease the amount of oxide formation that occurs, also resulting in minimization of the amount of the H adsorption reaction.

These phenomena are some of the reasons why CSC calculations overestimate the amount of charge that can be transferred during neural stimulation pulsing and may help to explain why stimulation limits from the Shannon plot are usually lower than calculated CSCs for platinum. Assuming the potential window from OCP toward hydrogen evolution better represents the operational potential window during stimulation, the predicted CSC would be as low as 326 $\mu C/cm^2$ as demonstrated in the results of figure 3a. For this electrode size of 44×10^{-3} cm^2 with a limiting factor of k=1.75 (a common imposed limit for platinum), the Shannon plot would constrain stimulation to charge densities below 36 $\mu C/cm^2$, an order of magnitude below that predicted by the CSC. Hence, other factors must account for the

discrepancy in addition to the ones observed in this study. Future studies could focus on how kinetics of the electrochemical reactions affect charge transfer during fast stimulation pulses.

Acknowledgments

References

1. Shannon RV. A model of safe levels for electrical stimulation. IEEE Transactions on Biomedical Engineering. 1992; 39:424–6. [PubMed: 1592409]

2. McCreery DB, Agnew WF, Yuen TGH, Bullara L. Charge density and charge per phase as cofactors in neural injury induced by electrical stimulation. Biomedical Engineering, IEEE Transactions on. 1990; 37:996–1001.

3. Beebe X, Rose TL. Charge injection limits of activated iridium oxide electrodes with 0.2 ms pulses in bicarbonate buffered saline. IEEE Transactions on Biomedical Engineering. 1988; 35:494–5. [PubMed: 3397105]

4. Cogan SF, Plante TD, Ehrlich J. Sputtered iridium oxide films (SIROFs) for low-impedance neural stimulation and recording electrodes. 26th Annual International Conference of the IEEE Engineering in Medicine and Biology Society. 2004; 2:4153–6.

5. Rose TL, Kelliher EM, Robblee LS. Assessment of capacitor electrodes for intracortical neural stimulation. Journal of Neuroscience Methods. 1985; 12:181–93. [PubMed: 2984478]

6. Nguyen-Vu TDB, Chen H, Cassell AM, Andrews RJ, Meyyappan M, Li J. Vertically Aligned Carbon Nanofiber Architecture as a Multifunctional 3-D Neural Electrical Interface. IEEE Transactions on Biomedical Engineering. 2007; 54:1121–8. [PubMed: 17554831]

7. Piret G, Hébert C, Mazellier J, Rousseau L, Scorsone E, Cottance M, Lissorgues G, Heuschkel MO, Picaud S, Bergonzo P, Yvert B. 3D-nanostructured boron-doped diamond for microelectrode array neural interfacing. Biomaterials. 2015; 53:173–83. [PubMed: 25890717]

8. Tykocinski M, Duan Y, Tabor B, Cowan RS. Chronic electrical stimulation of the auditory nerve using high surface area (HiQ) platinum electrodes. Hearing Research. 2001; 159:53–68. [PubMed: 11520634]

9. Park S, Song YJ, Boo H, Chung TD. Nanoporous Pt Microelectrode for Neural Stimulation and Recording: In Vitro Characterization. J. Phys. Chem. C. 2010; 114:8721–6.

10. Petrossians A, Whalen JJ, Weiland JD, Mansfeld F. Electrodeposition and Characterization of Thin-Film Platinum-Iridium Alloys for Biological Interfaces. J. Electrochem. Soc. 2011; 158:D269–76.

11. Li M, Zhou Q, Duan YY. Nanostructured porous platinum electrodes for the development of low-cost fully implantable cortical electrical stimulator. Sensors and Actuators B. Chemical. 2015; 221:179–86.

12. Cui X, Hetke JF, Wiler JA, Anderson DJ, Martin DC. Electrochemical deposition and characterization of conducting polymer polypyrrole/PSS on multichannel neural probes. Sensors and Actuators A. Physical. 2001; 93:8–18.

13. Cui X, Martin DC. Electrochemical deposition and characterization of poly(3,4-ethylenedioxythiophene) on neural microelectrode arrays. Sensors and Actuators B. Chemical. 2003; 89:92–102.

14. Green RA, Hassarati RT, Goding JA, Baek S, Lovell NH, Martens PJ, Poole-Warren LA. Conductive Hydrogels: Mechanically Robust Hybrids for Use as Biomaterials. Macromol. Biosci. 2012; 12:494–501. [PubMed: 22344960]

15. Hassarati RT, Dueck WF, Tasche C, Carter PM, Poole-Warren LA, Green RA. Improving Cochlear Implant Properties Through Conductive Hydrogel Coatings. IEEE Transactions on Neural Systems and Rehabilitation Engineering. 2014; 22:411–8. [PubMed: 24608692]

16. Cogan SF, Guzelian AA, Agnew WF, Yuen TGH, McCreery DB. Over-pulsing degrades activated iridium oxide films used for intracortical neural stimulation. Journal of Neuroscience Methods. 2004; 137:141–50. [PubMed: 15262054]

17. Norlin A, Pan J, Leygraf C. Investigation of Electrochemical Behavior of Stimulation/Sensing Materials for Pacemaker Electrode Applications I. Pt, Ti, and TiN Coated Electrodes. J. Electrochem. Soc. 2005; 152:J7–15.

18. Green RA, Hassarati RT, Bouchinet L, Lee CS, Cheong GLM, Yu JF, Dodds CW, Suaning GJ, Poole-Warren LA, Lovell NH. Substrate dependent stability of conducting polymer coatings on medical electrodes. Biomaterials. 2012; 33:5875–86. [PubMed: 22656446]

19. Baek S, Green RA, Poole-Warren LA. The biological and electrical trade-offs related to the thickness of conducting polymers for neural applications. Acta Biomaterialia. 2014; 10:3048–58. [PubMed: 24726957]

20. Brummer SB, Turner MJ. Electrochemical Considerations for Safe Electrical Stimulation of the Nervous System with Platinum Electrodes. IEEE Transactions on Biomedical Engineering. 1977; BME-24:59–63.

21. Brummer SB, Turner MJ. Electrical Stimulation with Pt Electrodes: II-Estimation of Maximum Surface Redox (Theoretical Non-Gassing) Limits. IEEE Transactions on Biomedical Engineering. 1977; BME-24:440–3.

22. Rose TL, Robblee LS. Electrical stimulation with Pt electrodes. VIII. Electrochemically safe charge injection limits with 0.2 ms pulses (neuronal application). IEEE Transactions on Biomedical Engineering. 1990; 37:1118–20. [PubMed: 2276759]

23. Cogan SF. Neural Stimulation and Recording Electrodes. Annual Review of Biomedical Engineering. 2008; 10:275–309.

24. Enyo, M. Hydrogen Electrode Reaction on Electrocatalytically Active Metals. In: Conway, BE.Bockris, JOM.Yeager, E.Khan, SUM., White, RE., editors. Comprehensive Treatise of Electrochemistry. Springer; US: 1983. p. 241-300.

25. Frumkin, AN. Advances in Electrochemistry and Electrochemical Engineering: Vol. 3: Electrochemistry. New York: Interscience Publishers/Wiley & Sons; 1963. Hydrogen Overvoltage and Adsorption Phenomena.

26. Brummer SB. The Use of Large Anodic Galvanostatic Transients to Evaluate the Maximum Adsorption on Platinum from Formic Acid Solutions. J. Phys. Chem. 1965; 69:562–71.

27. Biegler T, Rand DAJ, Woods R. Limiting oxygen coverage on platinized platinum; Relevance to determination of real platinum area by hydrogen adsorption. Journal of Electroanalytical Chemistry and Interfacial Electrochemistry. 1971; 29:269–77.

28. Hudak EM, Mortimer JT, Martin HB. Platinum for neural stimulation: voltammetry considerations. J. Neural Eng. 2010; 7:026005.

29. Robblee, LS., Rose, TL. The Electrochemistry Of Electrical Stimulation. Proceedings of the Twelfth Annual International Conference of the IEEE Engineering in Medicine and Biology Society, 1990; Proceedings of the Twelfth Annual International Conference of the IEEE Engineering in Medicine and Biology Society; 1990. p. 1479-80.

30. Zeitler S, Wendler-Kalsch E, Preidel W, Tegeder V. Corrosion of platinum electrodes in phosphate buffered saline solution. Materials and Corrosion. 1997; 48:303–10.

31. Hibbert DB, Weitzner K, Carter P. Voltammetry of Platinum in Artificial Perilymph Solution. J. Electrochem. Soc. 2001; 148:E1–7.

32. Musa S, Rand DR, Bartic C, Eberle W, Nuttin B, Borghs G. Coulometric Detection of Irreversible Electrochemical Reactions Occurring at Pt Microelectrodes Used for Neural Stimulation. Anal. Chem. 2011; 83:4012–22. [PubMed: 21545093]

33. Weremfo A, Carter P, Hibbert DB, Zhao C. Investigating the Interfacial Properties of Electrochemically Roughened Platinum Electrodes for Neural Stimulation. Langmuir. 2015; 31:2593–9. [PubMed: 25669232]

34. Kumsa DW, Bhadra N, Hudak EM, Kelley SC, Untereker DF, Mortimer JT. Electron transfer processes occurring on platinum neural stimulating electrodes: a tutorial on the i (V e) profile. J. Neural Eng. 2016; 13:052001. [PubMed: 27518125]

35. Frumkin, A., Krishtalik, L. Hydrogen Overvoltage and Adsorption Phenomena. Wiley; 1961.

36. Shao M, Liu P, Adzic RR. Superoxide Anion is the Intermediate in the Oxygen Reduction Reaction on Platinum Electrodes. J. Am. Chem. Soc. 2006; 128:7408–9. [PubMed: 16756272]

37. Jin W, Du H, Zheng S, Xu H, Zhang Y. Comparison of the Oxygen Reduction Reaction between NaOH and KOH Solutions on a Pt Electrode: The Electrolyte-Dependent Effect. J. Phys. Chem. B. 2010; 114:6542–8. [PubMed: 20411967]

38. Zhang C, Fan FF, Bard AJ. Electrochemistry of Oxygen in Concentrated NaOH Solutions: Solubility, Diffusion Coefficients, and Superoxide Formation. J. Am. Chem. Soc. 2009; 131:177–81. [PubMed: 19063634]

39. Pourbaix MJN, Van Muylder J, de Zoubov N. Electrochemical Properties of the Platinum Metals. Platinum Metals Review. 1959; 3:47–53.

40. García N, Climent V, Orts JM, Feliu JM, Aldaz A. Effect of pH and Alkaline Metal Cations on the Voltammetry of Pt(111) Single Crystal Electrodes in Sulfuric Acid Solution. ChemPhysChem. 2004; 5:1221–7. [PubMed: 15446746]

41. Robblee LS, McHardy J, Marston JM, Brummer SB. Electrical stimulation with Pt electrodes. V. The effect of protein on Pt dissolution. Biomaterials. 1980; 1:135–9. [PubMed: 7470564]

42. Bagotzky VS, Vassilyev YB, Weber J, Pirtskhalava JN. Adsorption of anions on smooth platinum electrodes. Journal of Electroanalytical Chemistry and Interfacial Electrochemistry. 1970; 27:31–46.

43. Angerstein-Kozlowska H, Conway BE, Sharp WBA. The real condition of electrochemically oxidized platinum surfaces: Part I: Resolution of component processes. Journal of Electroanalytical Chemistry and Interfacial Electrochemistry. 1973; 43:9–36.

44. Nart FC, Iwasita T. On the adsorption of sulfate species on polycrystalline platinum: An FTIR study in fluoride base electrolyte. Journal of Electroanalytical Chemistry and Interfacial Electrochemistry. 1991; 308:277–93.

45. Paulissen VB, Korzeniewski C. IR spectroscope as a probe of bisulfate absorption at platinum electrodes under aqueous electrochemical conditions: elimination of bulk interference by using a thin layer flow cell. Journal of Electroanalytical Chemistry. 1993; 351:329–35.

46. Savinova DV, Molodkina EB, Danilov AI, Polukarov YM. Surface and Subsurface Oxygen on Platinum in a Perchloric Acid Solution. Russian Journal of Electrochemistry. 2004; 40:683–7.

47. Rand DAJ, Woods R. The rest potential of platinum electrodes in oxygensaturated 1 M sulphuric acid. Journal of Electroanalytical Chemistry and Interfacial Electrochemistry. 1973; 47:353–61.

48. Novak DM, Conway BE. Competitive adsorption and state of charge of halide ions in monolayer oxide film growth processes at Pt anodes. J. Chem. Soc., Faraday Trans. 1. 1981; 77:2341–59.

49. Conway BE. Electrochemical oxide film formation at noble metals as a surface-chemical process. Progress in Surface Science. 1995; 49:331–452.

50. Jerkiewicz G, Vatankhah G, Lessard J, Soriaga MP, Park Y. Surface-oxide growth at platinum electrodes in aqueous H2SO4: Reexamination of its mechanism through combined cyclic-voltammetry, electrochemical quartz-crystal nanobalance, and Auger electron spectroscopy measurements. Electrochimica Acta. 2004; 49:1451–9.

51. Kodera F, Kuwahara Y, Nakazawa A, Umeda M. Electrochemical corrosion of platinum electrode in concentrated sulfuric acid. Journal of Power Sources. 2007; 172:698–703.

52. Hoare JP. Rest Potentials in the Platinum-Oxygen-Acid System. J. Electrochem. Soc. 1962; 109:858–65.

53. Merrill DR, Stefan IC, Scherson DA, Mortimer JT. Electrochemistry of Gold in Aqueous Sulfuric Acid Solutions under Neural Stimulation Conditions. J. Electrochem. Soc. 2005; 152:E212–21.

54. Beckman JS, Koppenol WH. Nitric oxide, superoxide, and peroxynitrite: the good, the bad, and ugly. American Journal of Physiology - Cell Physiology. 1996; 271:C1424–37.

55. Pacher P, Beckman JS, Liaudet L. Nitric Oxide and Peroxynitrite in Health and Disease. Physiological Reviews. 2007; 87:315–424. [PubMed: 17237348]

56. Szabó C, Ischiropoulos H, Radi R. Peroxynitrite: biochemistry, pathophysiology and development of therapeutics. Nat Rev Drug Discov. 2007; 6:662–80. [PubMed: 17667957]

57. Llopis J, Sancho A. Electrochemical Corrosion of Platinum in Hydrochloric Acid Solutions. J. Electrochem. Soc. 1961; 108:720–6.

58. Littauer EL, Shreir LL. Anodic polarization of platinum in sodium chloride solutions. Electrochimica Acta. 1966; 11:527–36.

59. Komanicky V, Chang KC, Menzel A, Markovic NM, You H, Wang X, Myers D. Stability and Dissolution of Platinum Surfaces in Perchloric Acid. J. Electrochem. Soc. 2006; 153:B446–51.

60. Bockris JOM, Azzam AM. The kinetics of the hydrogen evolution reaction at high current densities. Trans. Faraday Soc. 1952; 48:145–60.

61. Wicke E, Weblus B. Polarisationskapazität, Adsorption und Überspannung des Wasserstoffs an Platin. Zeitschrift für Elektrochemie, Berichte der Bunsengesellschaft für physikalische Chemie. 1952; 56:169–76.

62. Yeager E, Oey TS, Hovorka F. The Effect of Ultrasonic Waves on Hydrogen Overvoltage. J. Phys. Chem. 1953; 57:268–75.

63. Bockris JOM, Ammar IA, Huq AKMS. The Mechanism of the Hydrogen Evolution Reaction on Platinum, Silver and Tungsten surfaces in Acid Solutions. J. Phys. Chem. 1957; 61:879–86.

64. Will FG, Knorr CA. Untersuchung des Auf- und Abbaues von Wasserstoff- und Sauerstoffbelegungen an Platin mit einer neuen instationären Methode. Zeitschrift für Elektrochemie, Berichte der Bunsengesellschaft für physikalische Chemie. 1960; 64:258–69.

65. Anson FC. Effect of Surface Oxidation on the Behavior of Platinum Electrodes. The Fe(III)-Fe(II) Couple in Sulfuric Acid and Perchloric Acid. Anal. Chem. 1961; 33:934–9.

66. Anson FC, King DM. Effect of Surface Oxidation and Platinization on the Behavior of Platinum Electrodes. Reduction of Vanadium(V) and Iodate. Anal. Chem. 1962; 34:362–5.

67. Shibata S. The Activation of Platinum Electrodes by Preoxidation. Bull. Chem. Soc. Jpn. 1963; 36:525–7.

68. French WG, Kuwana T. Lifetime of Activated Platinum Surface. J. Phys. Chem. 1964; 68:1279–84.

69. Wagner FT, Moylan TE. Hydrogen chloride adsorption and coadsorption with hydrogen or water on platinum (111). Surface Science. 1989; 216:361–85.

70. Li N, Lipkowski J. Chronocoulometric studies of chloride adsorption at the Pt(111) electrode surface. Journal of Electroanalytical Chemistry. 2000; 491:95–102.

71. Bernabeu P, Tamisier L, De Cesare A, Caprani A. Study of the adsorption of albumin on a platinum rotating disk electrode using impedance measurements. Electrochimica Acta. 1988; 33:1129–36.

72. Alsabet M, Grden M, Jerkiewicz G. Comprehensive study of the growth of thin oxide layers on Pt electrodes under well-defined temperature, potential, and time conditions. Journal of Electroanalytical Chemistry. 2006; 589:120–7.
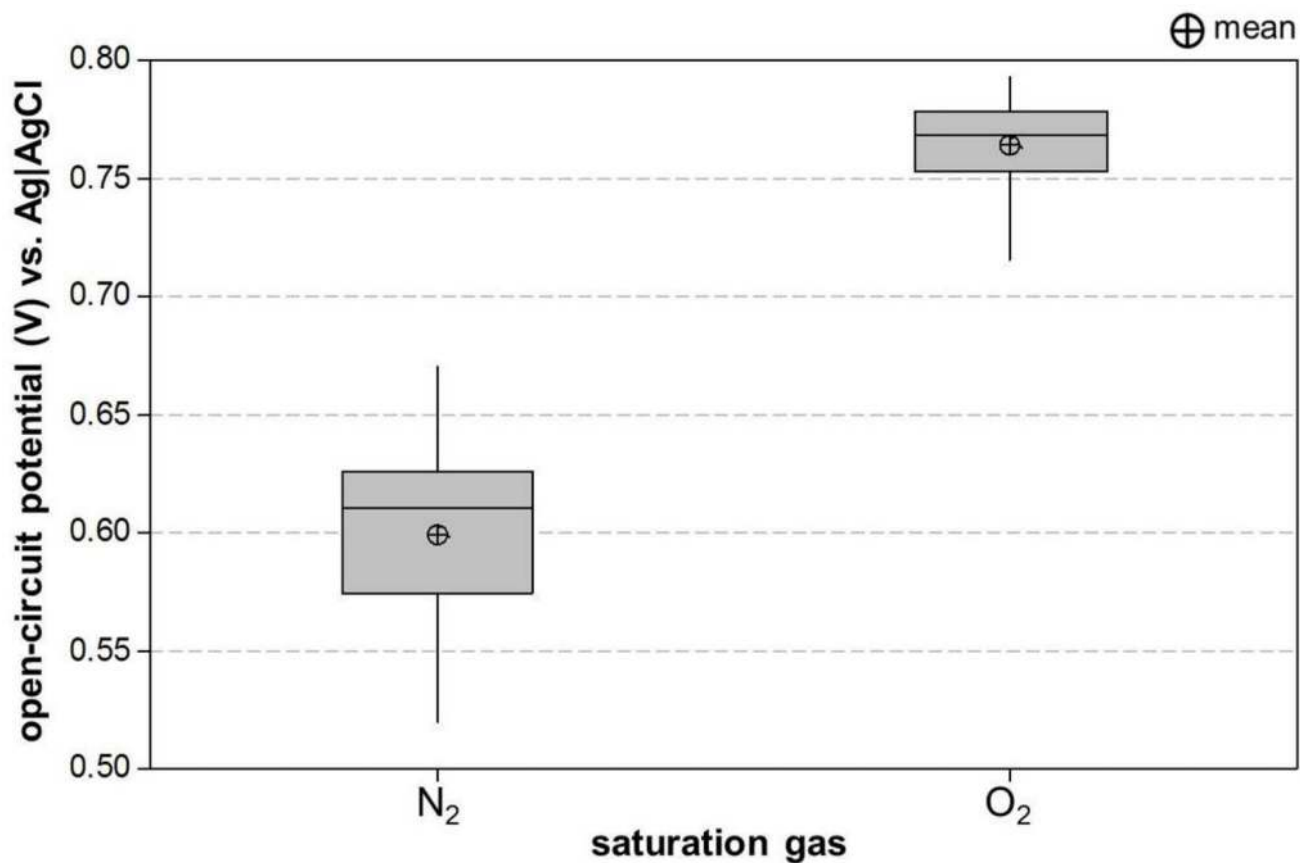
Figure 1.
Box-whisker plot of open-circuit potential for a platinum electrode submerged in 0.15 M H_2SO_4 saturated with either N_2 or O_2 gas. Mean OCP for each gas is denoted with a crosshair. The interquartile range box represents the central 50% of the data points in each group. The median is indicated by the horizontal line through the box. The whiskers extend to the upper- and lower-most data points in each group.
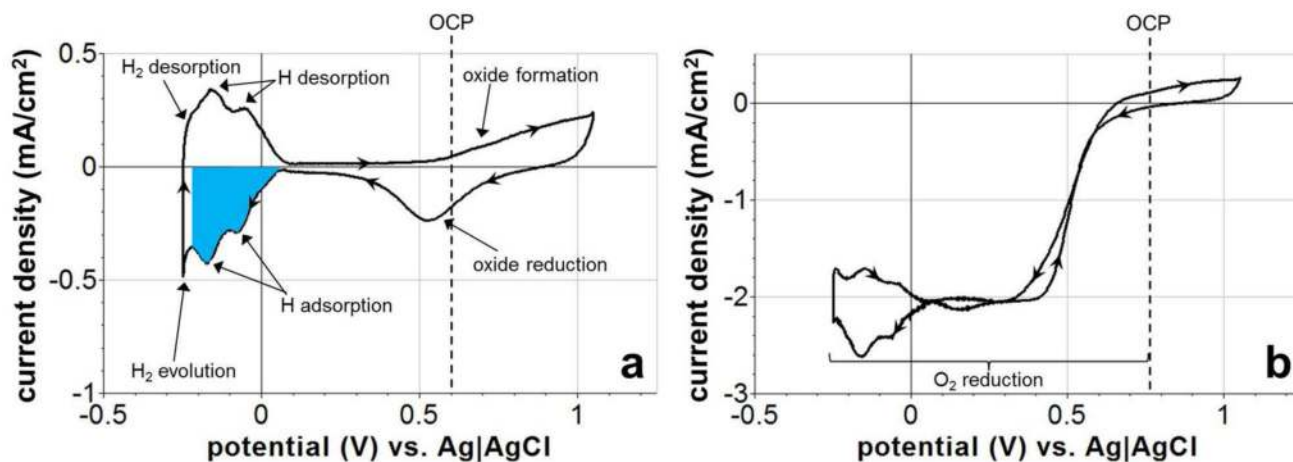
Figure 2.
Steady-state i-E curves of platinum in N_2-saturated (a) and O_2-saturated (b) 0.15 M H_2SO_4 from −0.25 V to +1.25 V vs. Ag|AgCl. (a) The N_2-saturated i-E curve exhibits typical platinum electrochemistry: oxide formation, oxide reduction, atomic hydrogen (H) adsorption, H desorption, and molecular hydrogen (H_2) evolution. Cathodic charge transfer associated with double-layer charging and the hydrogen adsorption reactions (blue shaded area) was 698 μC/cm^2. (b) The O_2-saturated i-E curve shows the same reactions as the N_2 case, plus O_2 reduction at potentials negative of the OCP (+0.76 V).
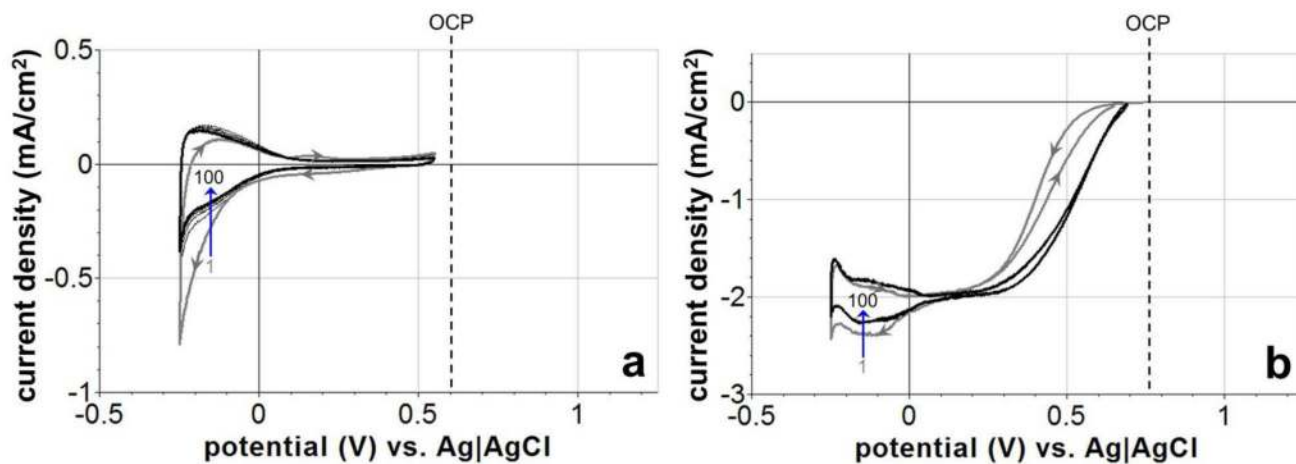
Figure 3.

i-E curves of platinum in N_2-saturated (a) and O_2-saturated (b) 0.15 M H_2SO_4 between −0.25 V to +0.55 V (near OCP); the sequence of the cycles is indicated with an arrow labeled from the first to the 100th cycle. The first cycle is shown in gray, intermediate cycles are thin black traces, and the last cycle of the progression is in bold black. Cycling through this potential range more accurately reflects the potential window platinum electrodes encounter during neural stimulation pulsing. Over the first 100 cycles, charge densities associated with double-layer charging and hydrogen adsorption steadily decrease from 438 $\mu C/cm^2$ to 326 $\mu C/cm^2$.
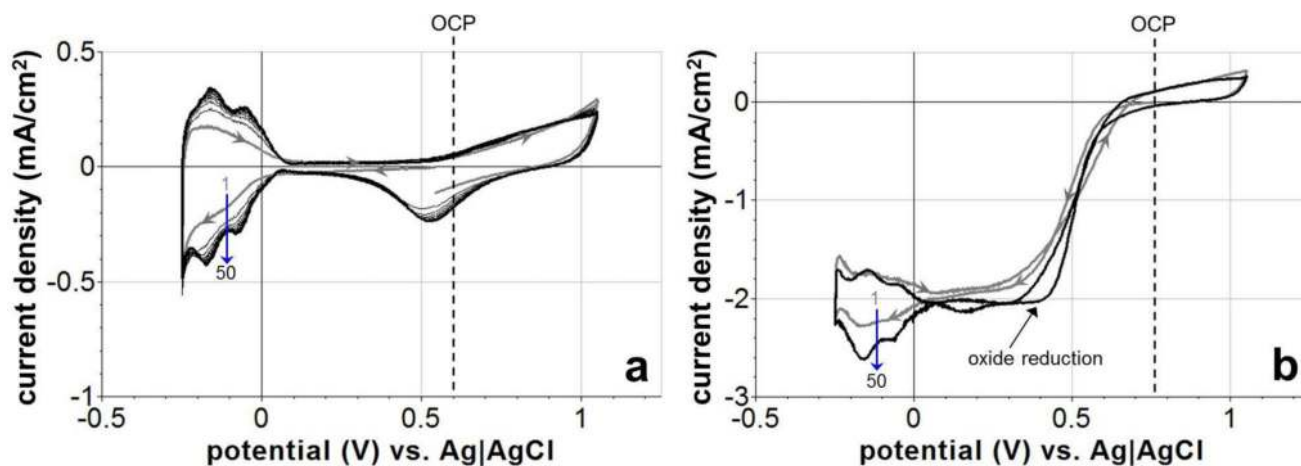
Figure 4.

i-E curves of platinum in N_2-saturated (a) and O_2-saturated (b) 0.15 M H_2SO_4 from −0.25 V to +1.25 V. (a) The first cycle exhibits a hydrogen adsorption level similar to the last cycle of figure 3a. When polarized repetitively into the oxide formation region (> +0.55 V), H adsorption current increases and clear peaks begin to form. Only by scanning into the oxide formation region did platinum achieve a charge density of 698 $\mu C/cm^2$ for the H adsorption region. (b) Current for H adsorption increased to a steady-state level after the 50 cycles in O_2-saturated H_2SO_4.
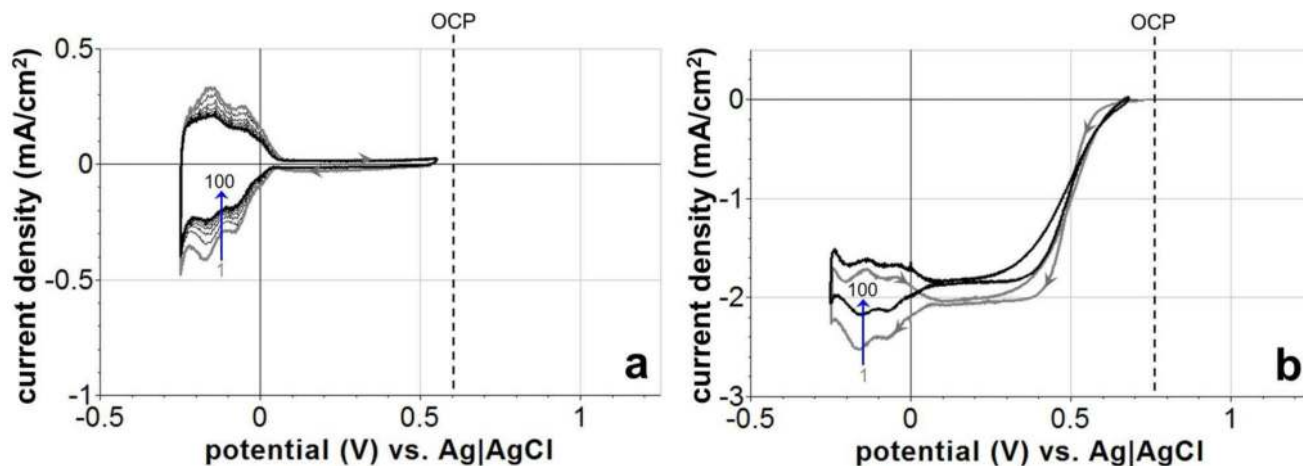
Figure 5.
i-E curves of previously scanned platinum in N_2-saturated (a) and O_2-saturated (b) 0.15 M H_2SO_4 over a narrow potential range from −0.25 V to near OCP. The first cycle is shown in gray, intermediate cycles are thin black traces, and the last cycle of the progression is bold black. (a) For early cycles, clear peaks for H adsorption and desorption are observed. As scanning progresses, the peaks become less well defined and current decreases. By the last cycle, cathodic charge density for the H adsorption region decreased from 690 $\mu C/cm^2$ to 435 $\mu C/cm^2$. (b) A decrease in charge transfer for H adsorption was also observed in the O_2-saturated case.
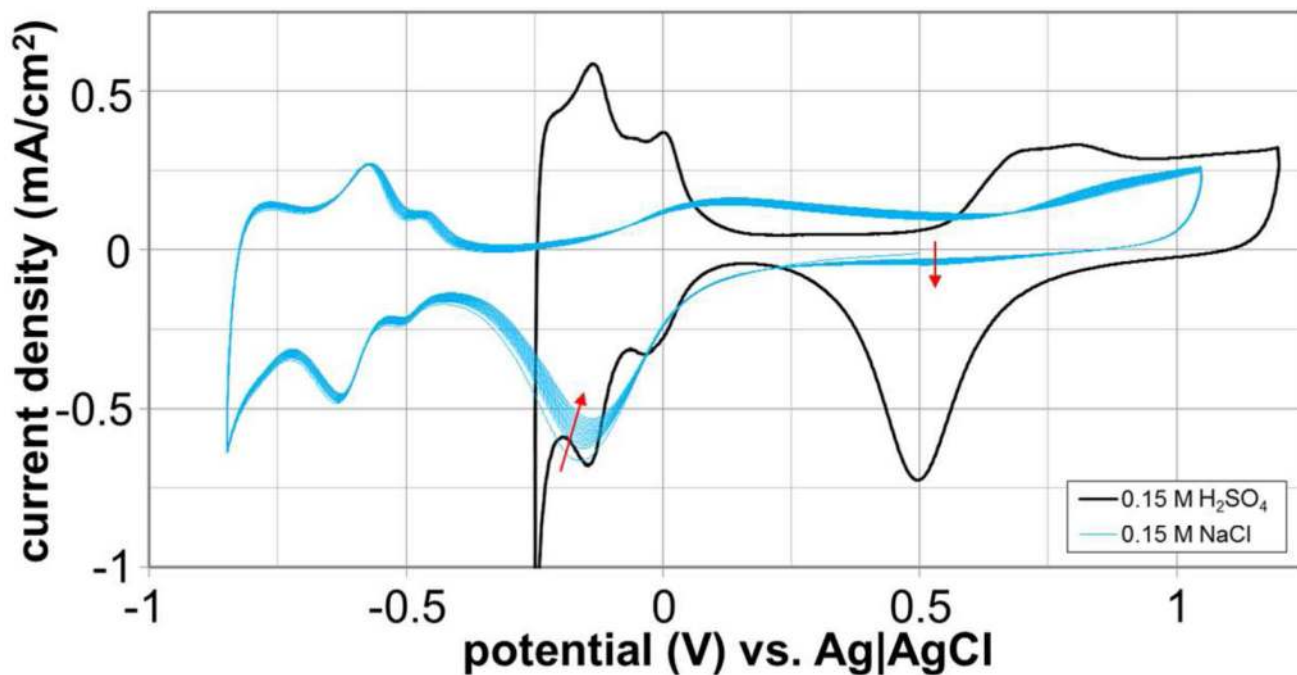
Figure 6.
The i-E curve of a platinum disk electrode in a 0.15 M NaCl electrolyte (blue trace) continuously changes with repeated cycling, unlike the repeatable i-E curve of Pt in sulfuric acid that exhibits a steady curve after repeated cycling (black trace). The oxide reduction current decreases with time and an additional small reduction peak begins to appear near +0.50 V (red arrows). The negative limit of the i-E curves in unbuffered NaCl is shifted 0.55 V negative of the i-E curve in sulfuric acid due to the difference in pH between the two electrolytes.
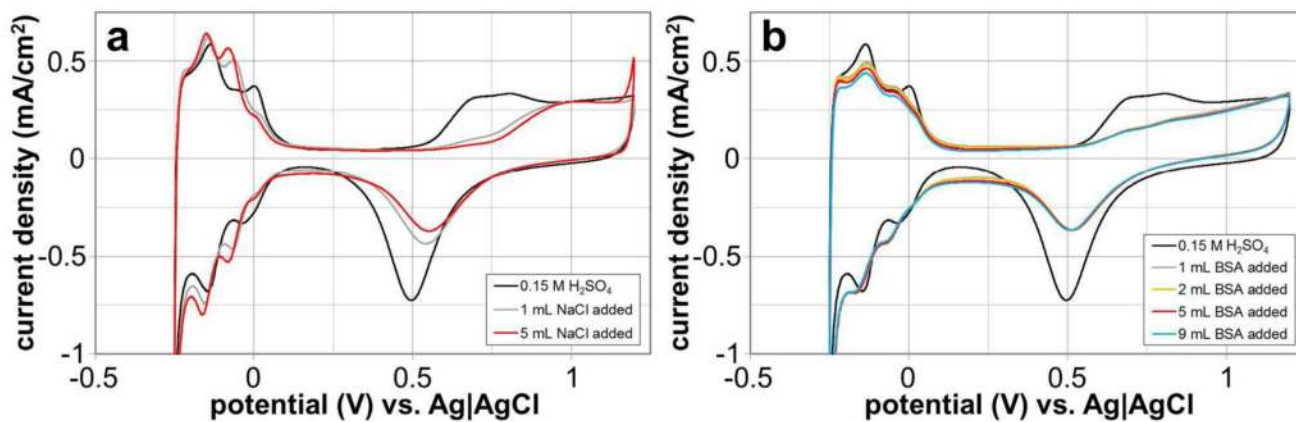
Figure 7.
The effect of adding Cl$^-$ to 0.15 M H$_2$SO$_4$ electrolyte is shown in part (a). The oxide formation and reduction current is depressed, and changes in hydrogen adsorption current occur starting with a 1 mL addition of NaCl. The effect of adding BSA to the electrolyte is shown in part (b). Suppression of the oxide formation current and changes in hydrogen adsorption are observed.

Table 1

Open-Circuit Potential (vs. Ag|AgCl) of a platinum electrode in N_2-saturated and O_2-saturated 0.15 M H_2SO_4.

Saturation Gas	Mean OCP (V)	Standard Deviation (V)
N_2 (N=13)	0.60	0.038
O_2 (N=8)	0.76	0.023